1-1-2005

Polystyrene Nanocomposites based on Carbazole-Containing Surfactants

Grace Chigwada
Marquette University

David D. Jiang
Marquette University

Charles A. Wilkie
Marquette University, charles.wilkie@marquette.edu

Accepted version. *Thermochimica Acta,* Volume 436, Issues 1-2, pp 113-121 (October, 2005). DOI:

Thermochimica Acta, Vol. 436, No. 1-2 (October 1, 2005): 113-121. DOI.

Polystyrene Nanocomposites Based on Carbazole-Containing Surfactants

Grace Chigwada
Department of Chemistry, Marquette University, Milwaukee, WI
David D. Jiang
Department of Chemistry, Marquette University, Milwaukee, WI
Charles A. Wilkie
Department of Chemistry, Marquette University, Milwaukee, WI

Abstract

New organically-modified clays containing a carbazole unit were prepared and the number of long alkyl chains on the surfactant was varied. The clay was used to prepare polystyrene nanocomposites by both bulk polymerization and melt blending. The dispersion of these clays in the polymer matrix was evaluated using X-ray diffraction (XRD) and transmission electron microscopy (TEM). The thermal stability of the clays and the nanocomposites were analyzed by thermogravimetric analysis (TGA) while the fire properties were evaluated by cone calorimetry. If more than two alkyl chains were present, the gallery spacing is apparently overcrowded, leading to poor dispersion. Bulk polymerization gave nanocomposites with better dispersion and reduced flammability when compared to the melt blending process.

Keywords

Nanocomposites, Polystyrene, Carbazole, Fire retardancy

1. Intoduction

Polymer-clay nanocomposites have attracted a significant amount of interest, due to the enhancement in barrier properties [1], [2], fire retardancy [3], [4], mechanical properties [5], [6] and the heat distortion temperature [7]. The physical and chemical properties of nanocomposites have stimulated fundamental and applied research in this field; particularly because of their high performances at very low clay loading [8], [9].

The combination of a nano-dimensional material with a polymer may yield either a micrcomposite, also known as an immiscible nanocomposite, in which the clay is acting as filler and is not dispersed at the nanometer level, or a true nanocomposite. If the registry between the clay layers is maintained, the material is described as intercalated, while, if this registry is lost, the material is described as delaminated, also known as exfoliated [10]. Intercalated, delaminated and immiscible, or any combination of these, can coexist. In some instances, notably barrier and mechanical properties, delamination gives clearly superior properties while for fire retardancy, there does not appear to be any difference between intercalation and delamination.

The compatibility, and thus the quality of the nano-dispersion, between the polymer and the clay have been improved by developing new surfactants for the modification of the clay. [10], [11], [12], [13] The commercial clay, Cloisite 10A (Southern Clay Products, Inc.), contains a single benzene ring and, in recent work from this laboratory, a clay containing a naphthyl substituent was described and this gives better dispersion in polystyrene than is obtained with the Cloisite 10A clay [14]. In this study, a larger substituent, carbazole, was placed on the ammonium cation and the number of long chains was varied to ascertain how the dispersion of the clay in the polymer is effected and how this may influence fire retardancy.

2. Experimental

2.1. Materials

The majority of chemicals used in the study, including carbazole, tetrabutylammonium bromide, styrene, polystyrene, ethyl acetate, tetrahydrofuran (THF), *N*,*N*-dimethylhexadecylamine, didecylmethylamine, and benzoyl peroxide (BPO), were obtained from the Aldrich Chemical Company. Montmorillonite was kindly provided by Southern Clay Products, Inc.

2.2. Preparation of bromo-alkyl carbazoles, 5AC and 10AC

The bromo-alkyl carbazoles, containing a 5-carbon chain, 5AC, and a 10-carbon chain, 10AC, were prepared by a phase transfer catalysis reaction as outlined in literature [15], [16], [17], [18].

2.3. Preparation of the alkyl carbazole salt (10AC salt)

The 10AC salt was prepared by the combination of 10AC and *N*,*N*-dimethylhexadecylamine. In a 250-ml 2-neck flask, equipped with an addition funnel and a condenser, was placed 10 g (26 mmol) 10AC in 100 ml ethyl acetate and this was stirred for a few minutes using a magnetic stirrer. To this was gradually added 8.5 g (31 mmol) *N,N*-dimethylhexadecylamine and the reaction mixture was refluxed for 24 h. The mixture was cooled to room temperature, the solvent removed and the sample recrystallized from ether. The reaction was quantitative; 17.2 g of product was recovered. ^{1}**H** $CDCl_3$:

δ8.080–8.117 (dd, J_1 = 7.32, J_2 = 3.60 2H), δ7.379–7.467 (m, 4H), δ7.189–7.242 (m, 2H), δ4.259–4.326 (q, J_1 = 6.90, J_2 = 3.45 2H), δ3.337–3.3411 (m, 4H), δ2.221 (s, 6H), δ1.778–1.906 (m, 2H), δ1.189–1.295 (br, 42H), δ0.856–0.901 (t, J_1 = 13.6, J_2 = 6.6 3H).

The same procedure was used to prepare the 5AC Salt. ^{1}**H** $CDCl_3$: δ8.071–8.098 (d, J = 8.10 2H), δ7.292–7.492 (m, 4H), δ7.140–7.222 (m, 2H), δ4.286–4.334 (t, J_1 = 14.40, J_2 = 6.90 1H), δ4.203–4.250 (t, J_1 = 14.10 J_2 = 6.98 1H), δ3.315–3.421 (m, 4H), δ2.16 (s, 6H), δ1.814–1.942 (m, 2H), δ1.216–1.264 (br, 32H), δ.837–.881 (t, J_1 = 13.20 J_2 = 6.30 3H).

2.4. Preparation of the di-alkyl carbazole salt (10ACDD salt)

The combination of the 10AC with didecylmethylamine was performed following the same procedure except that the solvent used was ethanol and the mixture was refluxed for 48 h. The solvent was removed on a vacuum pump and the product was recrystallized from ether. The yield was 97%; 34.4 g of product was recovered. ^{1}**H** $CDCl_3$: δ8.093–8.119 (d, J = 7.84, 2H), δ7.313–7.499 (m, 4H), δ7.257–7.212 (m, 2H), δ4.306–4.353 (t, J_1 = 14.10 J_2 = 7.24 1H), δ4.222–4.269 (t, J_1 = 14.10 J_2 = 5.40 1H), δ3.396–3.441 (t, J_1 = 13.5 J_2 = 6.60 4H), δ3.335–3.380 (t, J_1 = 13.5, J_2 = 6.90 2H), δ2.081 (s, 3H), δ1.831–1.940 (m, 4H), δ1.120–1.362 (br, 44H), δ0.993–1.041 (t, J_1 = 14.4 J_2 = 6.90 6H).

2.5. Organic modification of the clay

A portion of the ammonium salts prepared above was dissolved in 100 ml of THF while the clay was dispersed in 200 ml of 2:1 water:THF; a 10% excess of the ammonium salt, based on the CEC of the clay was used. These were mixed and stirred at room temperature for 24 h, followed by filtration and continuous washing with water until no chloride ion was detected using an aqueous silver nitrate solution. Three different clays were produced which have different organic contents, as would be expected since the molecular mass of the cation is varied; the 5AC clay is 28% organic substituent, while 10AC is 37% organic and 10ACDD is 52% organic.

2.6. Preparation of polystyrene-clay nanocomposites

Both bulk polymerization and melt blending processes were utilized for the preparation of nanocomposites, following the procedures outlined in the literature [19]. Briefly, bulk polymerization involves dispersing the clay in monomeric styrene, then adding initiator and carrying out the polymerization by heating. Melt blending was performed using a Brabender mixer for a fixed period of time, usually about 15 min at a temperature of about 180 °C.

2.7. Instrumentation

X-ray diffraction (XRD) measurements were performed using a Rigaku powder diffractometer with a Cu tube source (λ = 1.54 Å); generator tension was 50 kV at a current of 20 mA. Scans were taken from 2ϑ = 1.0–10, step size = 0.1 and scan time per step of 10 s using the high-resolution mode. Bright field transmission electron microscopy (TEM) images of the composites were obtained at 60 kV with a Zeiss 10c electron microscope. The samples were ultramicrotomed with a diamond knife on a Richert-Jung Ultra-Cut E microtome at room temperature to give ~70 nm thick section. The sections were transferred from the knife-edge to 600 hexagonal mesh Cu grids. Thermogravimetric analysis, TGA, was performed on a Cahn TG 131 unit under a flowing nitrogen atmosphere at a scan rate of 20 °C/min from 20 to 600 °C. All TGA experiments have been done in triplicate; the reproducibility of temperature is ±3 °C while amount of nonvolatile residue is reproducible to ±5%. Cone calorimeter measurements at 35 k/Wm^2 were performed using an Atlas Cone 2; the spark was continuous until the sample ignited. All samples were run in triplicate and the average value is reported. Results from cone calorimeter are generally considered to be reproducible to ±10% [20].

3. Results and discussion

Three different novel surfactants have been used in this study and their structures are shown in Fig. 1. In one case, 5AC, the substituents include a hexadecyl, two methyls and a carbazole with a 5-carbon linkage to the ammonium ion. The second compound, 10AC, contains in addition to the hexadecyl and methyls, a 10-carbon connector between the carbazole and the ammonium ion, while the third, 10ACDD, has two decyl chains, one methyl group and again a 10-carbon linker between the carbazole and the ammonium ion. Thus, 5AC contains one long chain and a carbazole while 10AC has two long chains and 10ACDD has three long chains. The objective is to evaluate nanocomposite formation and properties as a function of the substituents on the ammonium cation.

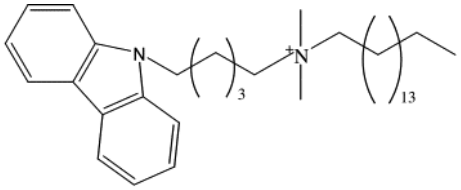

5AC salt

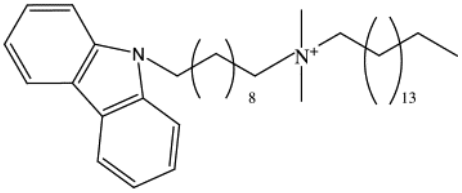

10AC Salt

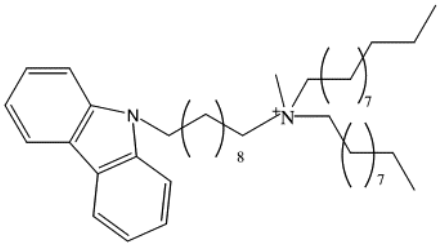

10ACDD Salt

Fig. 1. Carbazole-based salts used in this study.

3.1. X-ray diffraction (XRD) analysis

The d-spacing between the alumino-silicate layers for the organically-modified clays was measured by XRD and the results are shown in Table 1. It is clear from this data that a significant increase in the gallery spacing between the clay layers was observed for all the three organically-modified clays, compared to the sodium MMT clay. These clays were then used to prepare polystyrene-clay nanocomposites by in situ bulk polymerization and by melt blending. The dispersion of these clays in the polystyrene matrix was evaluated by X-ray diffraction and TEM.

Table 1. Summary for XRD analysis

Compound	**2ϑ**	**d-Spacing (nm)**
Sodium clay	7.9	1.1
5AC clay	3.0	3.0
PS + 3% 5AC clay, melt blending	2.4	3.7

PS + 5% 5AC clay, melt blending	2.5	3.5
PS + 10% 5AC clay, melt blending	2.6	3.4
PS + 1% 5AC clay, Bulk	2.5	3.5
PS + 3% 5AC clay, Bulk	2.6	3.4
PS + 5% 5AC clay, Bulk	2.5	3.5
10AC clay	3.0	3.0
PS + 3% 10AC clay, melt blending	2.6	3.4
PS + 5% 10AC clay, melt blending	2.6	3.4
PS + 10% 10AC clay, melt blending	2.6	3.4
PS + 3% 10AC clay, Bulk	2.8	3.2
PS + 5% 10AC clay, Bulk	2.8	3.2
PS + 7% 10AC clay, Bulk	2.8	3.2
10ACDD clay	3.2	2.8
PS + 3% 10ACDD clay, melt blending	3.2	2.8
PS + 5% 10ACDD clay, melt blending	3.2	2.8
PS + 3% 10ACDD clay, Bulk	3.1	2.9
PS + 5% 10ACDD clay, Bulk	3.2	2.8
PS + 7% 10ACDD clay, Bulk	3.2	2.8

Fig. 2, Fig. 3 and Table 1 give a summary of XRD data. There was a slight increase in the d-spacing associated with nanocomposite formation when both 5AC and 10AC clays were used, while 10ACDD did not show any increase, as has also been observed when other ammonium ions which contain three long chain substituents have been used [14]; this is likely a result of an overcrowded gallery space. Since peaks are observed at a lower value of 2ϑ, intercalation is assumed but this must be evaluated by transmission electron microscopy. In the case of the 10ACDD salt, the lack of any change likely indicates that styrene has not penetrated the gallery space and an immiscible system may be expected.

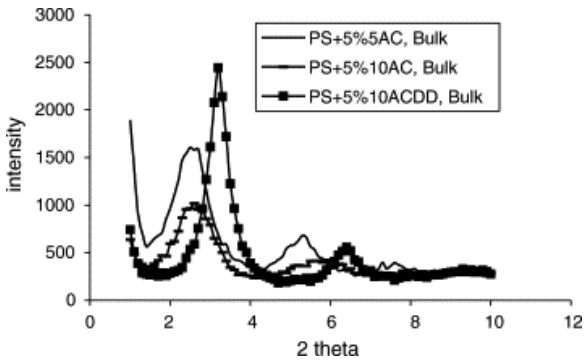

Fig. 2. XRD for PS + clay nanocomposites prepared by bulk polymerisation.

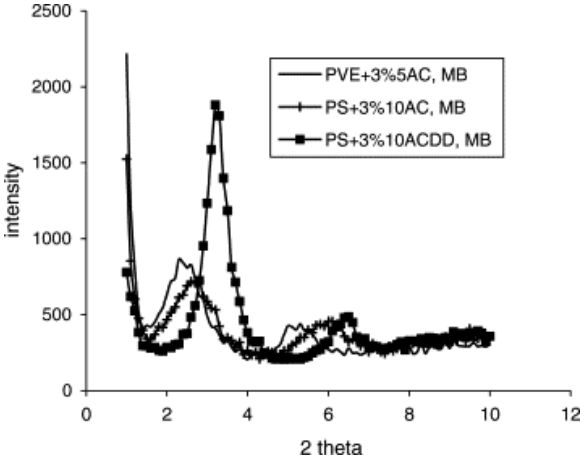

Fig. 3. XRD for PS + clay nanocomposites prepared by melt blending.

3.2. Transmission electron microscopy (TEM)

In order to confirm the type of hybrid structure that has been formed, TEM images were obtained and these are shown in Fig. 4, Fig. 5, Fig. 6, Fig. 7, Fig. 8, Fig. 9. From the low magnification images, one can see that excellent dispersion results for all systems prepared by bulk polymerization, while for those prepared by melt blending, the presence of clay tactoids is quite evident and these must be described as immiscible systems. The poorer dispersion for melt blended samples might be due to the fact that there is crowding in the gallery space due to the presence of the bulky carbazole group and an increased number of long alkyl chains; it is much easier for monomer to penetrate the crowded gallery space than for the polymer. From the high magnification images of the bulk polymerized samples, one can see individual clay layers in the case of 5AC, which may be best described as a mixed intercalated—delaminated system; while for 10AC, no individual clays layers are obvious and this may be a mixed immiscible-intercalated system while for 10ACDD, a system which did not give an expanded d-spacing in the XRD, shows individual clay layers as well as tactoids and, apparently, a mixed immiscible; intercalated, delaminated system. This result for the 10ACDD system is not at all what was expected from the XRD data and shows the difficulty of relying only on XRD information to attempt to describe nanocomposite formation.

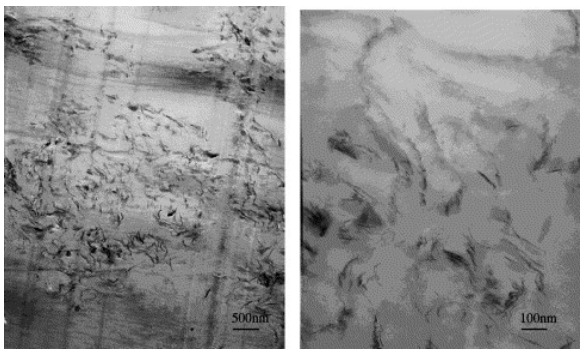

Fig. 4. TEM images for bulk polymerized styrene with 3% 5AC clay.

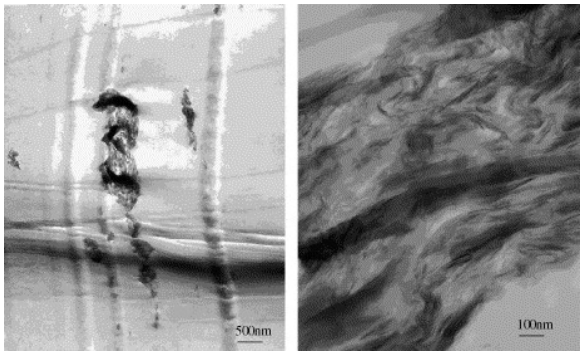

Fig. 5. TEM images for melt blended polystyrene with 3% 5AC clay.

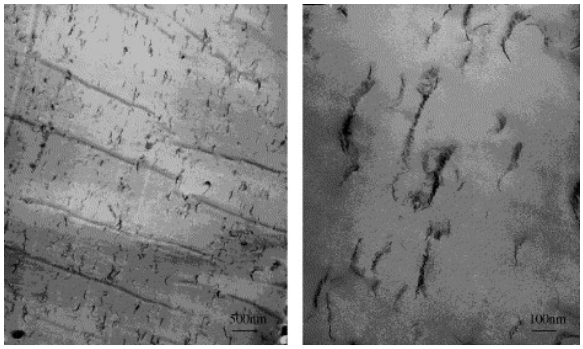

Fig. 6. TEM images for bulk polymerized styrene with 3% 10AC clay.

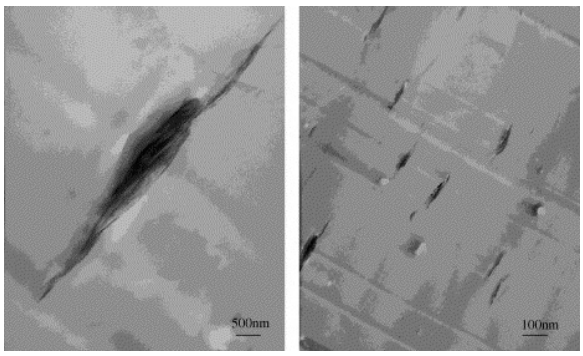

Fig. 7. TEM images for melt blended polystyrene with 3% 10AC clay.

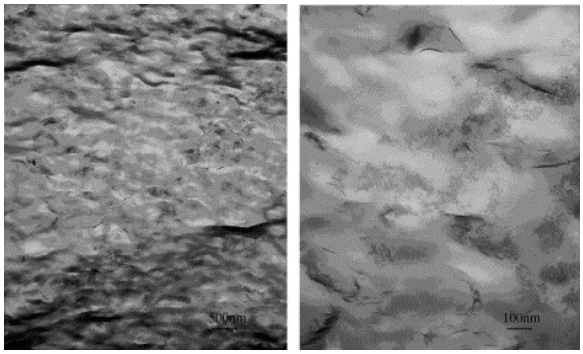

Fig. 8. TEM images for bulk polymerized styrene with 3% 10ACDD clay.

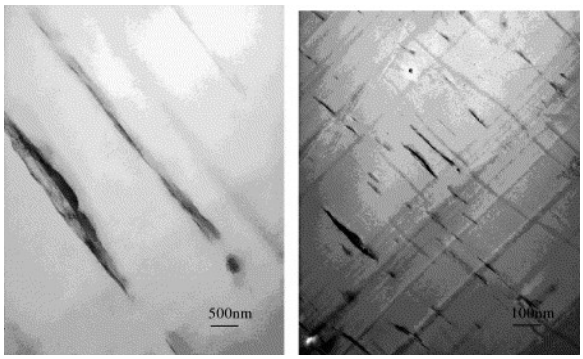

Fig. 9. TEM images for melt blended polystyrene with 3% 10ACDD clay.

3.3. Thermogravimetric analysis (TGA)

TGA is widely used to characterize the thermal stability of polymers. The parameters that are of interest include the onset temperature of the degradation, usually evaluated as the temperature at which 10% degradation occurs, T_{10}, the 50% degradation temperature, T_{50}, and the amount of non-volatile residue that remains at 600 °C, denoted as char.

Fig. 10 shows the TGA curves for the three clays used in this study. It is apparent from this study that there is significant variation in the initial degradation temperatures for the three clays with 10AC clay giving the highest onset temperature while 10ACDD gives the lowest onset of degradation temperature. The char gives a measure of the inorganic content; 5AC has the highest inorganic content while 10ACDD has the least, in agreement with the length and number of chains of the cation.

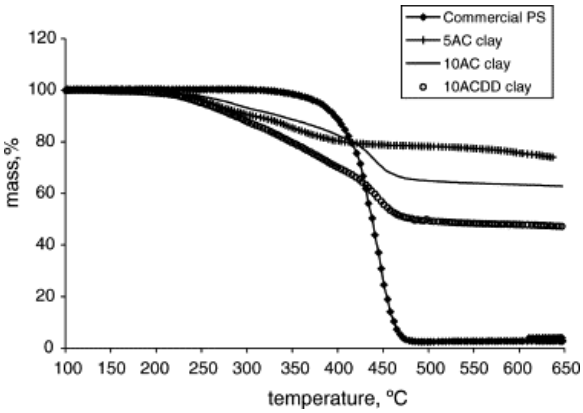

Fig. 10. TGA curves for polystyrene and the three new clays used in this study.

Fig. 11, Fig. 12 show the thermal degradation curves for the nanocomposites while Table 2 gives a summary of all the data collected. From the table, it can be concluded that for 5AC and 10AC clays, samples prepared by bulk polymerization show increased thermal stability compared to virgin polystyrene. The onset temperature may show a small increase for bulk polymerization of both 5AC and 10AC while the thermal stability of the 10ACDD nanocomposite is clearly lower. The temperature at which 50% degradation occurs increases for both 5AC and 10AC and is comparable to that of polystyrene for 10ACDD. The 10ACDD clay is not as thermally stable as the others, which means that the nanocomposites are also less thermally stable. There is little, if any, change in the degradation temperatures for melt blending, which supports that these are immiscible materials in which the clay is acting simply as filler. Polystyrene nanocomposites typically exhibit a substantial increase in both the onset and mid-point temperatures of degradation, with an increase of 30–50 °C being somewhat common. [19] For all the systems, the amount of char increases as the amount of clay increases.

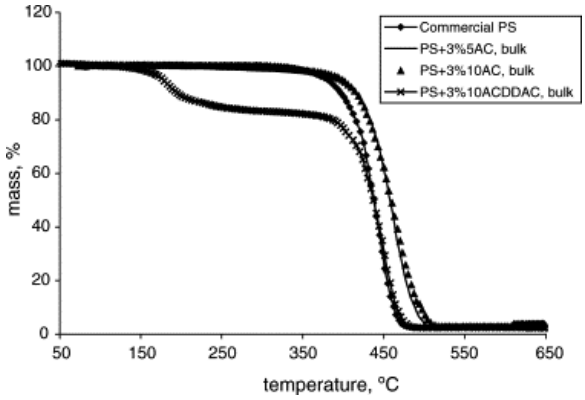

Fig. 11. TGA analysis for nanocomposites prepared by bulk polymerisation.

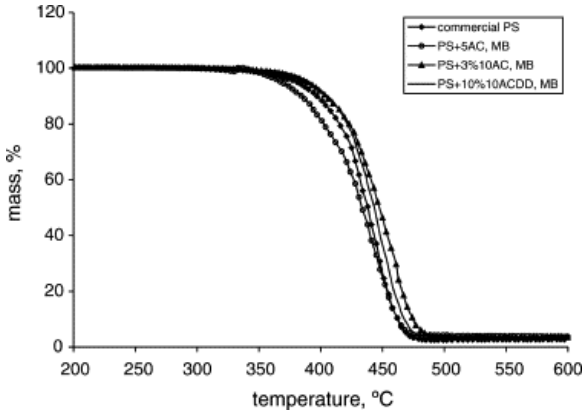

Fig. 12. TGA analysis for nanocomposites prepared melt blending.

Table 2. TGA data for polystyrene nanocomposites from the carbazole-containing surfactants

Sample	T_{10}	T_{50}	**% Char**
Commercial PS	409	442	0
5AC clay	325	–	72
10AC clay	335	–	63
10ACDD clay	281	477	48
PS + 3% 5AC, melt blending	382	433	5
PS + 5% 5AC, melt blending	395	433	7
PS + 10% 5AC, melt blending	400	449	11
PS + 1% 5AC, Bulk	392	441	2
PS + 3% 5AC, Bulk	413	458	3
PS + 5% 5AC, Bulk	416	462	6
PS + 1% 10AC, Bulk	409	453	3
PS + 3% 10AC, Bulk	419	459	3
PS + 5% 10AC, Bulk	411	460	4
PS + 3% 10AC, melt blending	403	446	5
PS + 5% 10AC, melt blending	403	442	5
PS + 10% 10AC, melt blending	409	452	8
PS + 3% 10ACDD, melt blending	408	445	3
PS + 5% 10ACDD, melt blending	411	448	5
PS + 5% Cloisite 10A, melt blending	400	452	6

PS + 5% Cloisite 30B, melt blending	419	463	6

The last two entries in Table 2 show the data obtained when commercially available clays were used. The initial degradation temperature, T_{10}, for the nanocomposites prepared by the commercial clays is comparable to that obtained with the new clays. On the other hand the nanocomposites prepared by bulk polymerization are comparable for all the clays, which means these new clays have the potential to be used where all the other clays are used.

3.4. Cone calorimetry

The parameters that may be evaluated from cone calorimetry include the heat release rate, and especially its peak value, PHRR; the times to ignition and peak heat release rate; specific extinction area (SEA), a measure of smoke; and the mass loss rate. One of the parameters that have been given special attention in fire retardancy is the peak heat release rate, PHRR, as this gives information about the size of the fire and thus the approximate fire hazard. In the literature, it has been shown that nanocomposite formation gives rise to the maximum reduction in PHRR while a microcomposite gives essentially no reduction. [21], [22]. The time to ignition is a measure of the ease of ignition of a material, and nanocomposite formation, as well as the presence of other additives, has been associated with shorter times to ignition than in the virgin polymer. The specific extinction area is a measure of the amount of smoke that is evolved during the combustion, while the mass loss rate is correlated with the reduction in PHRR, i.e. the reduction in PHRR occurs because of a change in the mass loss rate. Nanocomposites also tend to release the same amount of heat, the total heat released, THR, as does the virgin polymer, which means that everything ultimately burns, but it will take longer in the case of a nanocomposite.

The data for the nanocomposites prepared using 5AC and 10AC clays will be compared first. The difference between these two clays is that one of the clays (10AC clay) contains five more carbon atoms in one of the chains. For both clays, it was observed from the HRR curves, Fig. 13, Fig. 14, Fig. 15, Fig. 16, that bulk polymerization resulted in samples with lower PHRRs than those prepared by melt blending. The PHRR for 5AC is slightly lower than that of 10AC, implying slightly better fire retardant action. All of the other data, including the total heat released, mass loss rate, time to ignition and the specific extinction area, are comparable for the two systems. The length of the connector between the carbazole and the ammonium ion does not appear to be important for changes in cone calorimetric parameters.

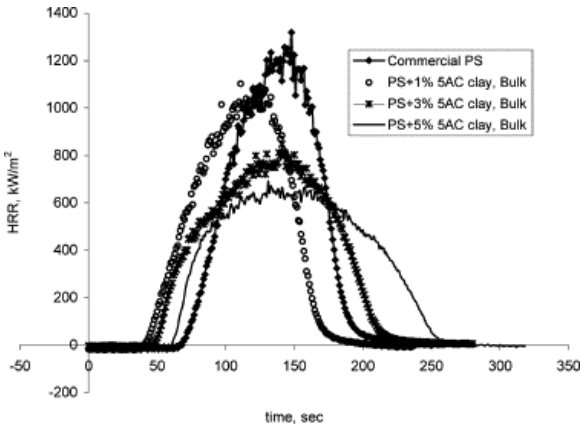

Fig. 13. HRR curves for PS + 5AC clay nanocomposites, bulk.

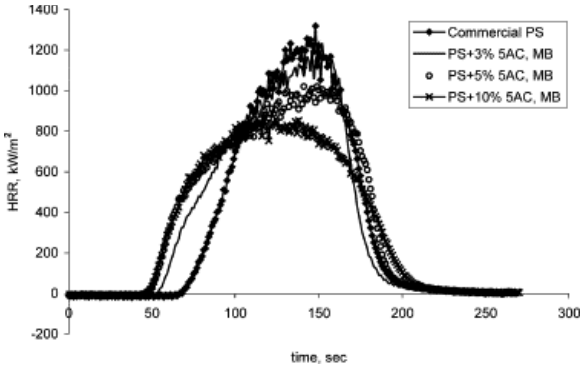

Fig. 14. HRR curves for PS + 5AC clay nanocomposites, melt blending.

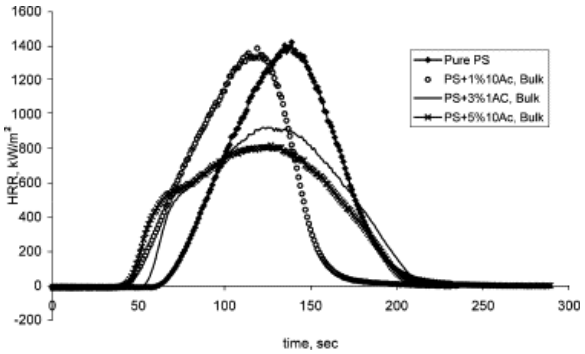

Fig. 15. HRR curves for PS + 10AC clay nanocomposites, bulk.

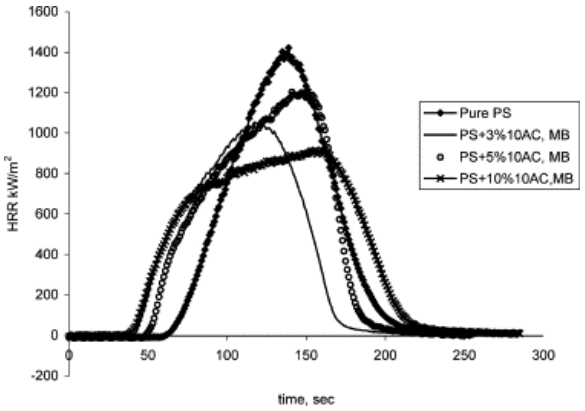

Fig. 16. HRR curves for PS + 10AC clay nanocomposites, melt blending.

A comparison of the data for 10AC and 10ACDD will evaluate the effect of the additional chain on the cone parameters. From the XRD analysis, the peak for the 10ACDD clay and the nanocomposites prepared with this clay appeared at the same position, which might suggest that the polymer does not penetrate into the gallery space. TEM images for the bulk-polymerized samples showed good dispersion and the cone data shows a substantial reduction in PHRR, which is typically a sign of good nano-dispersion. Comparable reductions in PHRR were observed with both 10AC and 10ACDD clays and the results are shown in Fig. 15, Fig. 16, Fig. 17 and Table 3. For the 10ACDD system, samples prepared by melt blending did not give a good reduction in PHRR, suggesting the formation of an immiscible system, in agreement with the TEM images. As with all the other clays that have been used to prepare styrene nanocomposites, clays that contain a carbazole group resulted in formation of nanocomposites with shorter times to ignition and no change in the total heat released. It is apparent from these data that all three of the clays give good nano-dispersion and that the number of long

chains does not have an effect upon the properties of nanocomposites prepared by bulk polymerization.

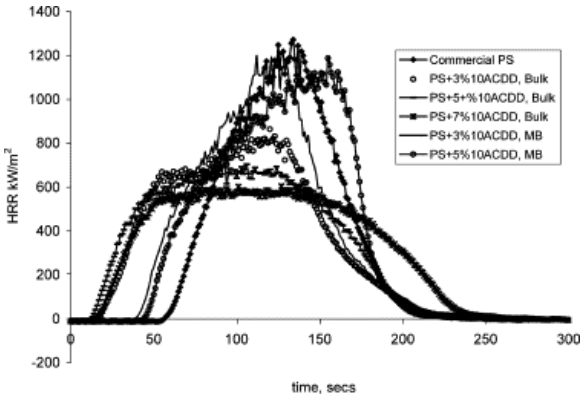

Fig. 17. HRR curves for PS + 10ACDD clay nanocomposites, bulk and melt blending.

Table 3. Cone calorimetric data for polystyrene nanocomposite at 35 kW/m^2

Sample	**t_{ign}[a] (s)**	**PHRR[a] (kW/m^2; % reduction)**	**t_{PHRR}[a] (s)**	**THR[a] (MJ/m^2)**	**MLR[a] (g/stm^2)**	**SEA[a] (m^2/kg)**
PS	61 ± 2	1376 ± 124	142 ± 14	95 ± 5	24 ± 3	1203 ± 54
+1% 5AC, Bulk	39 ± 4	1254 ± 142 (9)	125 ± 12	89 ± 5	25 ± 2	1125 ± 144
+3% 5AC, Bulk	43 ± 8	827 ± 61 (40)	129 ± 15	88 ± 1	19 ± 1	1297 ± 279
+5% 5AC, Bulk	52 ± 5	693 ± 38 (50)	132 ± 5	86 ± 4	17 ± 0	1286 ± 61
+3% 5AC, melt blending	49 ± 3	1233 ± 11 (10)	156 ± 7	100 ± 5	26 ± 1	1097 ± 87
+5% 5AC, melt blending	47 ± 4	1023 ± 7 (26)	149 ± 7	99 ± 3	23 ± 1	1176 ± 69
+10% 5AC, melt blending	38 ± 5	889 ± 49 (35)	127 ± 9	92 ± 1	20 ± 1	1331 ± 41
+1% 10AC, Bulk	43 ± 5	1297 ± 129 (6)	122 ± 3	91 ± 2	23 ± 2	1359 ± 34
+3% 10AC, Bulk	46 ± 5	923 ± 36 (33)	120 ± 8	85 ± 7	19 ± 2	1372 ± 37
+5% 10AC, Bulk	40 ± 4	828 ± 49 (40)	122 ± 7	86 ± 5	17 ± 0	1418 ± 43
+3% 10AC, melt blending	37 ± 6	1062 ± 38 (23)	134 ± 13	99 ± 10	21 ± 2	1245 ± 27
+5% 10AC, melt blending	42 ± 3	1159 ± 77 (16)	140 ± 3	100 ± 4	22 ± 1	1350 ± 53
+10% 10AC, melt blending	36 ± 2	945 ± 76 (31)	139 ± 16	99 ± 13	19 ± 1	1345 ± 76
+3% 10ACDD, Bulk	15 ± 1	864 ± 1 (37)	135 ± 20	99 ± 8	17 ± 1	1350 ± 22
+5% 10ACDD, Bulk	19 ± 1	695 ± 14 (49)	103 ± 13	98 ± 8	15 ± 1	1663 ± 170
+7% 10ACDD, Bulk	23 ± 1	626 ± 31 (55)	110 ± 25	90 ± 6	14 ± 0	1291 ± 32
+3% 10ACDD, melt blending	42 ± 7	1227 ± 35 (11)	126 ± 12	96 ± 2	21 ± 3	1327 ± 42
+5% 10ACDD, melt blending	44 ± 0	1193 ± 6 (13)	152 ± 6	106 ± 3	23 ± 1	1293 ± 50

[a] t_{ign}, time to ignition; PHRR, peak heat release rate; t_{PHRR}, time to PHRR; THR, total heat released; MLR, mass loss rate; SEA, specific extinction area.

4. Conclusions

Attaching alkyl groups in the form of long alkyl chains or as bulky groups, such as carbazole, improves the dispersion of the clay in the polymer but it is the inorganic portion of the clay that is responsible for reducing the peak heat release rate. Neither the time to ignition nor the total heat released are effected, compared to virgin polymer, by increasing the number of alkyl chains or incorporating larger groups like carbazole or naphthenate [14] groups attached to the modified clay. The presence of a large number of alkyl units increases crowding in the gallery space, which affects the dispersion of the clay in the polymer matrix and results in decreased thermal stability.

Acknowledgement

A portion of this work has been performed under the sponsorship of the Office of Naval Research under grant number N00014-03-1-0172 and this support is gratefully acknowledged.

References

[1] P.B. Messersmith, E.P. Giannelis. J. Polym. Sci. Part A: Polym. Chem., 33 (1995), p. 1047
[2] Y. Kojima, K. Fukumori, A. Usuki, A. Okada, T. Kurauchi. J. Mater. Sci. Lett., 12 (1993), p. 889
[3] J.W. Gilman, T. Kashiwagi, J.D. Lichtenham. SAMPE J., 33 (1997), p. 40
[4] J. Less, T. Takakoshi, E.P. Giannelis. Mater. Res. Soc. Symp. Proc., 457 (1997), p. 513
[5] K. Yano, A. Usuki, A. Okada, T. Kurauchi, O. Kamigaito. J. Polym. Sci. Part A: Polm. Chem., 31 (1993), p. 2493
[6] T. Lan, T.J. Pinnavaia. Chem. Mater., 6 (1994), p. 2216
[7] Xie.W. Wei, R. Xie, PanF P.W., D. Hunter, Koene B., L.S. Tan, R. Vaia. Chem. Mater., 14 (2002), pp. 4837-4845
[8] Y. Kojima, A. Usuki, M. Kawasumi, A. Okada, Y. Fukushima, T. Kurauchi, O. Kamigaito. J. Mater. Res., 8 (1993), pp. 1185-1189
[9] X. Kornmann, R. Thomann, R. Mulhaupt, J. Finter, L. Berglund. J. App. Polym. Sci., 86 (2002), p. 2643
[10] D. Wang, C.A. Wilkie. Polym. Degrad. Stab., 82 (2003), pp. 309-315
[11] S. Su, D.D. Jiang, C.A. Wilkie. Polym. Degrad. Stab., 83 (2004), pp. 321-331
[12] J. Zhang, C.A. Wilkie. Polym. Degrad. Stab., 83 (2004), pp. 301-307
[13] X. Zheng, C.A. Wilkie. Polym. Degrad. Stab., 82 (2003), pp. 441-450
[14] G. Chigwada, D.D. Jiang, C.A. Wilkie, in: C.A. Wilkie, G.L. Nelson (Eds.), Fire and Polymers, Materials and Concepts for Hazard Prevention, accepted for publication.
[15] X. Li, E.A. Mintz, X.R. Bu, O. Zehner, C. Bosshard, P. Gunter. Tetrahedron, 56 (2000), p. 5785
[16] X. Li, J. Wang, R. Mason, X.R. Bu, J. Harrison. Tetrahedron, 58 (2002), p. 3747
[17] R. Oshima, T. Wada, J. Kumanotani. J. Polym. Sci. Polym Chem., 22 (1984), p. 3135
[18] H. Katayama, S. Ito, M. Yamamoto. J. Phys. Chem., 96 (1992), p. 10115
[19] D. Wang, J. Zhu, Q. Yao, C.A. Wilkie. Chem. Mater., 14 (2002), p. 3837
[20] J.W. Gilman, T. Kashiwagi, M. Nyden, J.E.T. Brown, C.L. Jackson, S. Lomakin. S. Al-Maliaka, A. Golovoy, C.A. Wilkie (Eds.), Chemistry and Technology of Polymer Additives, London Blackwell Scientific (1998), pp. 249-265
[21] J.W. Gilman, T. Kashiwagi, M. Nyden, J.E.T. Brown, C.L. Jackson, S. Lomakin, E.P. Giannelis, E. Manias S. Al-Malaika, A. Golovoy, C.A. Wilkie (Eds.), Chemistry and Technology of Polymer Additives, Blackwell Scientific (1999), pp. 249-265
[22] S. Su, D.D. Jiang, C.A. Wilkie. J. Vinyl Add. Tech., 10 (2004), pp. 44-51